Power Transformer Protection Using a Multiregion Adaptive Differential Relay

Hamed Dashti and Majid Sanaye-Pasand, *Senior Member, IEEE*

***Abstract*—This paper presents a new adaptive approach to improve the performance of the power transformer differential relay. The proposed approach distinguishes internal faults and disturbances based on the differential current trajectory and adopted weighting factors depending on the differential current locus in the relay characteristic. The traditional dual-slope differential characteristic is divided into three operating regions with the corresponding weighting factors. Two other control regions, that is, inrush and current-transformer (CT) saturation detection regions are utilized to avoid maloperation of the proposed relay in the case of inrush and CT saturation conditions. Meanwhile, a combination of phase differential units is introduced as a new technique to decrease relay operation time. The proposed relay rapidly detects all studied internal faults, while it is stable during transformer energization and CT saturation due to external faults. A real 230/63-kV power transformer is simulated using PSCAD/EMTDC for evaluating the performance of the proposed relay. Extensive simulation studies show that the proposed approach results in a faster and smarter differential protection scheme.**

***Index Terms*—Current transformer (CT) saturation, inrush current, multiregion differential relay, power transformer protection.**

I. Introduction

A POWER transformer is one of the most important pieces of equipment in electrical systems. Thus, it should be protected by fast and accurate relays to prevent subsequent damage to the transformer due to internal faults. The low-impedance differential protection is one of the most widely used approaches for transformer protection. However, this relay may maloperate due to system disturbances, especially transformer inrush current and current-transformer (CT) saturation caused by an external fault. Therefore, it should be equipped with supplementary techniques to make it stable against such conditions [1], [2].

To avoid maloperation due to the inrush current, it is common practice to utilize the ratio of the second harmonic component of the differential current to its fundamental harmonic component. In this approach, the differential relay should be blocked when the current ratio exceeds a predefined set value [2]. Although this approach is widely utilized in commercial relays, it may impose an extra time delay on the operation of a differential relay due to the following points: 1) for the cases where the fault current includes a decaying dc component, the defined current ratio may temporarily become more than the set value, which blocks the differential relay for one or two cycles; 2) when a transformer with an internal fault is energized, the differential relay may be blocked for even ten cycles [3]; 3) reliable estimation of the first and second harmonic components can lead to about one cycle of extra delay. The associated delay may result in more damage to healthy parts of the transformer which increases the required repair time and expense. In addition, the current harmonic approach cannot detect large inrush currents which occur after energizing a transformer with a considerable remanent flux, especially for newly designed transformers [4], [5]. It is desirable to propose a new method which is not affected by these shortcomings.

Another challenge associated with the application of a differential relay is to guarantee its security against severe CT saturation during external faults. In such a condition, an artificial differential current is generated which may lead to relay maloperation. Since CT is usually not saturated during the first 3 ms after the fault inception, some techniques have been proposed to distinguish between internal and external faults in this time interval [6].

Recently, a variety of methods aimed at improved selectivity, sensitivity, and operation time of differential relays has been presented to overcome the related problems. These techniques include artificial neutral network (ANN) [7]–[9]; fuzzy logic [10]–[12]; and wavelet analysis [5], [13]–[15]. However, some of these methods: 1) need a large data set for training; 2) impose a high computational burden on the differential relay; and 3) depend on the transformer parameters or initial conditions [16], [17]. In addition, adaptive schemes have been utilized to enhance the digital relay performance (e.g., to achieve the optimal compromise between accuracy and speed of the relay [18]).

This paper highlights the fact that for the disturbances adversely affecting the differential relay, the calculated differential current has a certain trajectory and is located in a certain region of the relay characteristic. Thus, based on dividing the relay characteristic into several regions, a new adaptive strategy for the low-impedance differential relay is proposed in this paper. When the current trajectory enters the relay operational zone, a weighting factor (WF) is adopted to it depending on its region. When the summation of the weighted-points exceeds a certain prespecified value, the trip command is issued. Comprehensive time-domain simulation studies show that the proposed technique guarantees fast relay operation for internal fault cases and

Manuscript received March 19, 2013; revised July 06, 2013; accepted August 09, 2013. Date of publication October 17, 2013; date of current version March 20, 2014. This work was supported by the University of Tehran under Grant 8101064-1-06. Paper no. TPWRD-00321-2013.

The authors are with the Control and Intelligent Processing Center of Excellence, School of Electrical and Computer Engineering, College of Engineering, University of Tehran, Tehran 14395-515, Iran (e-mail: h.dashti@ut.ac.ir; msanaye@ut.ac.ir).

Color versions of one or more of the figures in this paper are available online at http://ieeexplore.ieee.org.

Digital Object Identifier 10.1109/TPWRD.2013.2280023

increases the relay security for inrush current and CT saturation cases.

II. Multiregion Differential Relay

Comprehensive time-domain simulation studies show that the calculated differential current for internal faults, inrush currents and CT saturations caused by external faults are located in different certain regions of the differential relay characteristic. This feature is used and a multiregion differential relay is suggested. The studied system and transformer are introduced in the following subsection. Afterwards, proposed different regions of the differential relay characteristic are introduced and discussed.

A. Studied System and Transformer

The studied system is composed of a 230/63 kV, YNd power transformer connected to a voltage source through a Thevenine impedance and the corresponding CTs. The parameters of the studied system are given in Appendix. The power transformer model is developed in the PSCAD/EMTDC environment [19] to evaluate the impact of faults on the differential relay [20]. Various internal faults, inrush currents, CT saturation cases and their combination can be studied using the modeled transformer.

To represent the hysteresis characteristic of the transformer magnetic core, a scalar model is adopted [21]. The model is capable of generating symmetric and asymmetric hysteresis minor loops, and also the remanent flux which is essential for inrush current calculations. In addition, to represent the actual system conditions, the knee point voltage of the corresponding CTs are calculated based on the CT requirement of a commercial relay [22]. The same scalar model is also utilized to model the CT core hysteresis characteristic to be able to consider the CT remanent flux. To provide more realistic results, the real hysteresis loop is measured using an appropriate experimental setup. Since a similar core material is usually used by both of the transformer and the CT manufacturers, only the CT hysteresis loop is measured. The measurement is carried out at the frequency of 1 Hz to decrease the resultant error caused by winding stray capacitances.

The schematic diagram of a YNd transformer is illustrated in Fig. 1 for which the currents at the low voltage (LV) terminals lags those of the high voltage (HV) terminals by 30 °. In such a transformer, two adjustments are required prior to calculation of the differential current including (i) compensation of phase-shift due to the YNd vector group and (ii) elimination of the zero-sequence current of the transformer [22]. For instance, the differential current of phase-A should be calculated by [23]

$$I_{\mathrm{diff}A} = \left|\frac{I_A - I_0}{I_N} + K_{CF}\frac{I_a - I_c}{\sqrt{3}I_n}\right| \quad (1)$$

where $\mathrm{I_A}$ is the calculated phasor of phase-A at the HV-side. $\mathrm{I_0}$ is the calculated zero-sequence current of HV-side by adding up the phase currents. $\mathrm{I_a}$ and $\mathrm{I_c}$ are the LV-side phasor currents of phase-a and phase-c, respectively. $\mathrm{I_N}$ and $\mathrm{I_n}$ are the rated currents of HV-side and LV-side, respectively. $\mathrm{K_{CF}}$ is a correction factor equal to the HV-side CT ratio over the LV-side one. It should be noted that the phasors are calculated based on the full cycle discrete Fourier transform (DFT) method with the sampling frequency of 1 kHz.

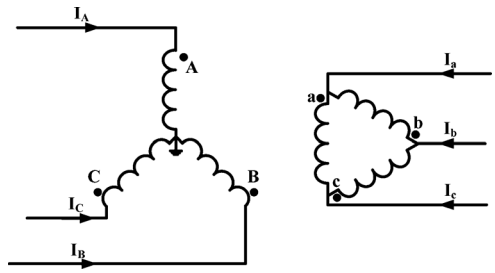

Fig. 1. Schematic diagram of a YNd11 power transformer.

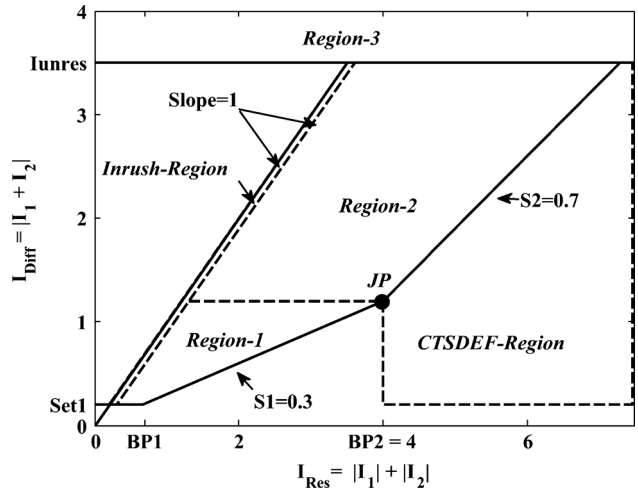

Fig. 2. Different regions of the proposed differential relay.

B. Regional Differential Relay Concept

Fig. 2 shows the multiregion differential characteristic used for the proposed relay. The settable parameters of the relay characteristic include: 1) two slopes which are set to $\mathrm{S1} = 0.3$ and $\mathrm{S2} = 0.7$; 2) two breaking points which are $\mathrm{BP1} = 0.67$ and $\mathrm{BP2} = 4$ p.u.; 3) minimum differential current as the pickup current, $\mathrm{Set}\ 1 = 0.2$ p.u.; and 4) unrestraint differential current $\mathrm{Iunres} = 3.5$ p.u.

It should be noted that selection of BP2 has an important role in the relay stability against CT saturation. According to the CT requirements, CT is not saturated for an external fault current of less than 2 p.u. [22]. Therefore, the corresponding restraint current BP2, that is, the sum of current absolute values, for CT saturation-free case is 4 p.u.

To guarantee secure operation of the differential relay, the current trajectory should remain in the operational zone for a certain amount of time. A fix time delay is usually used for the differential relay operation [22]–[26]. Whereas, the adverse effect of an internal fault on subsequent damages to the transformer and especially to the power system mainly depends on the severity of the fault current. In other words, low current faults usually lead to less subsequent damages and the relay can operate with longer delay, if necessary. On the other hand, higher fault currents should be cleared faster. In addition, the

relay must be secure for different transient phenomena, e.g., heavy external faults and inrush currents. The more the relay operating time, the more security of the relay.

The operation time of the proposed relay adaptively changes by using different weights for the samples entering the operational zone. Weighting the differential current samples is performed by introducing a number of regions. To cover all possible internal faults, the operational zone of the basic differential relay characteristic has been divided into three regions, namely Region-1, Region-2 and Region-3. Moreover, two control regions—Inrush-Region and CT saturation detection for external fault (CTSDEF)-Region—are applied to control stability of the proposed algorithm. These five regions, shown in Fig. 2, are chosen based on the level of the fault current and differential current trajectory for a variety of fault types.

III. Proposed Regions of Differential Relay

In this paper, different internal faults are categorized using the level of differential current and differential current trajectory in the relay characteristic. Based on the level of differential current, three groups of faults are considered: 1) mild internal faults; 2) heavy internal faults; and 3) severe internal faults. Hence, in the proposed relay, the differential characteristic operational zone has been divided into three operating regions as described in the following subsections.

A. Region of Mild Internal Faults

Various studies and simulations revealed that the low differential current owing to internal faults such as short circuited HV coil up to 20% of the winding, high impedance terminal faults and some LV turn-to-turn internal faults are located in the lowest part of differential characteristic, called Region-1. In addition, the differential current trajectory may enter this region due to the CT saturation for a low current external fault with high decaying dc time constant. Some typical fault trajectories are shown in Fig. 3. In this figure, AG means a phase A-to-ground internal fault and ac is a turn-to-turn internal fault on the delta winding between phases a and c. Also, % sign, R_f and $I_{diff\,A}$ denote the percentage of short circuited winding, fault resistance and differential current of phase-A, respectively.

B. Region of Heavy Internal Faults

Based on different simulation cases, it is concluded that a significant number of faults, such as faults on 20–45% of HV winding and 10–25% of LV winding, are located in the middle part of differential characteristic, called Region-2. Moreover, fictitious differential currents due to CT saturation for heavy through faults could also enter this region. A few of these events are plotted in Fig. 4.

C. Region of Severe Internal Faults

Similar to some relays, an unrestraint region on the top of the differential characteristic is considered to deal with severe internal faults. This region is not affected by fictitious differential currents due to inrush condition and CT saturation during external faults. Differential current of severe internal faults such as faults on 45%–100% of the HV winding, LV turn-to-turn faults including more than 25% of the winding and terminal

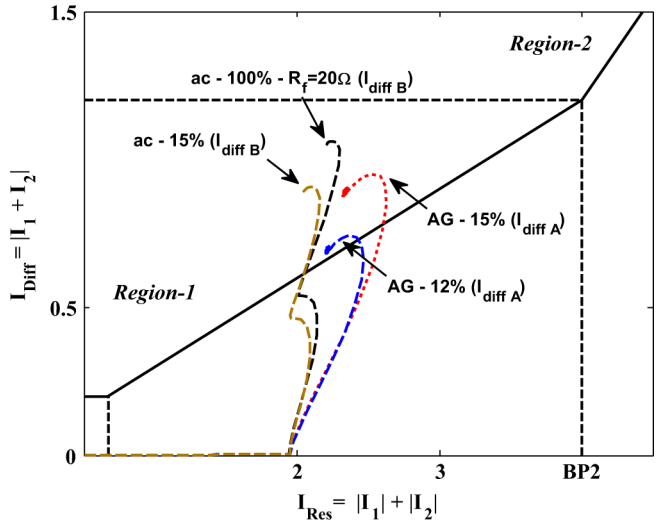

Fig. 3. Typical internal faults entering Region-1.

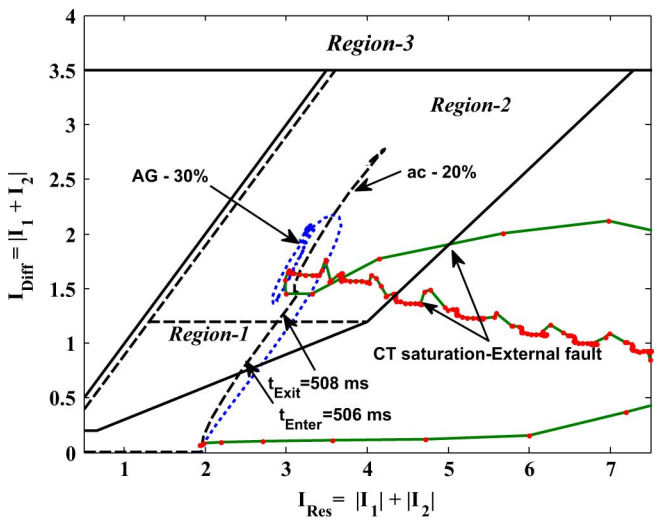

Fig. 4. Typical events entering Region-2.

low impedance faults are located in this region, Region-3. Some heavy internal fault trajectories are shown in Fig. 5. Region-3 should be immune against CT saturation caused by external faults. Simulation studies are performed to calculate the artificial differential current due to external faults for the transformer under study including the corresponding saturable CTs. As the worst possible case, the remanent flux of 80% is considered for a set of CTs at one side of the transformer; whereas, CTs of the other side are free from remanent flux. Under such a condition, severe CT saturation is occurred in only one set of CTs and causes the differential current of about 3.5 p.u. Thus the threshold of this region I_{unres} is set to 3.5 p.u.

D. Region of Saturated CT due to External Faults

Saturation of CTs due to high fault currents, large system time constants and high amounts of remanence are critical for external faults. Immediately after the external fault inception, the fault current increases severely thus producing a high restraint current (twice the through fault current). In the case of CT saturation, a fictitious differential current is produced and also the

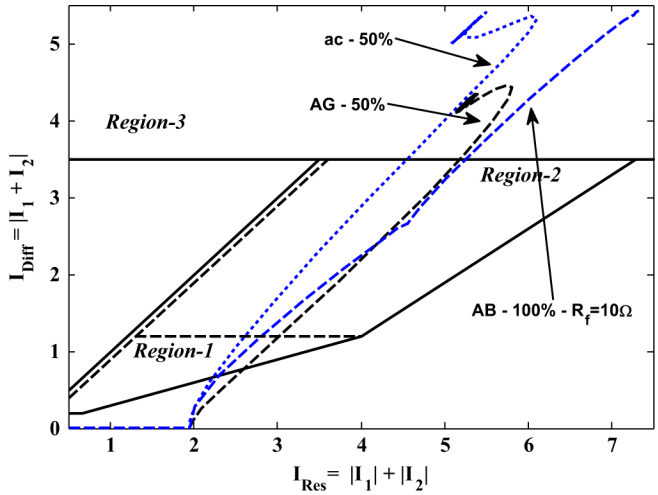

Fig. 5. Typical heavy internal faults entering Region-3.

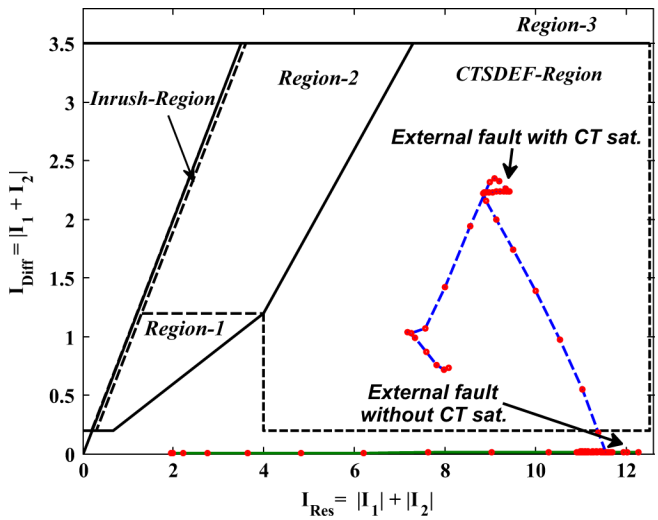

Fig. 6. External fault trajectories with/without CT saturation.

restraint current is reduced. If the I_{Diff}/I_{Res} ratio results in a point inside the operational zone, a trip signal would be issued if no special control is applied. External fault trajectory during CT saturation is located in the CTSDEF-Region in Fig. 6. This region is utilized to stabilize the proposed relay in the case of CT saturation for external faults .The CTSDEF-Region is activated when (2) is satisfied.

$$I_{\mathrm{Res}} \geq BP2 \text{ and } I_{\mathrm{Diff}} \geq \mathrm{Set1}. \tag{2}$$

E. Region of Inrush Currents

When switching unloaded transformers, high magnetizing inrush currents may occur which can result in high differential currents. In this condition, the current trajectory moves along a line bisecting the first quadrant. The worst inrush current occurs when power transformer core has high amount of remanence. By performing various studies, it is found that a parallelogram region shown in Fig. 2, that is, Inrush-Region, can

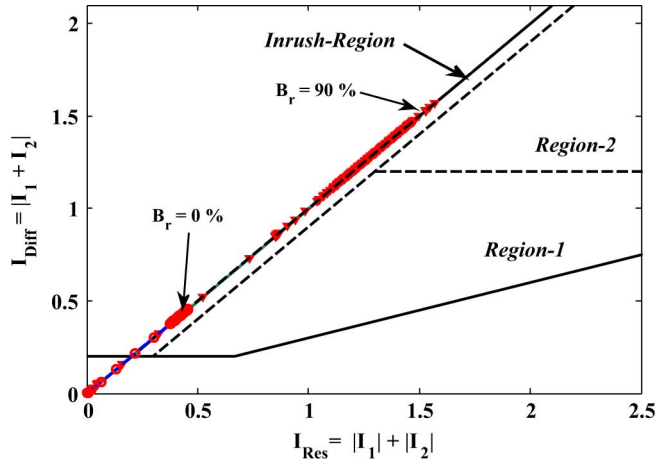

Fig. 7. Current trajectories of switching on a power transformer.

well detect the inrush energization cases. This region is not adversely affected by CT saturation during inrush current condition. Current trajectories for several transformer switching cases with/without remanence are depicted in Fig. 7. As shown, inrush current trajectories enter into Inrush-Region from the lower side of this region. This is a precondition of detecting inrush phenomenon. Failure to comply with this precondition, that is, entering the current trajectory into Region-1 or Region-2 and then moving into Inrush-Region from the diagonal side, is the evidence of occurrence of an internal fault. Under this circumstance, Region-1 and Region-2 are modified and expanded by merging Inrush-Region into them.

Calculation of the fundamental component of maximum possible inrush current is required for adjustment of the upper limit of Inrush-Region. The peak of inrush current, neglecting the system impedance, is calculated by (3)[27].

$$i_{\mathrm{peak}} = \frac{\sqrt{2}V}{\sqrt{(L\omega)^2 + R^2}} \left(\frac{2B_N + B_R - B_S}{B_N} \right) \tag{3}$$

where V, $L\omega$, R, B_N, B_R, and B_S are the applied voltage, air core impedance, total resistance, nominal flux density, remanent flux, and saturation flux density of the power transformer. The worst case, i.e., assuming B_R is equal to B_S and neglecting the resistive impedance, is considered to calculate the maximum peak of inrush current presented as

$$i_{\mathrm{peak}} \leq \frac{\sqrt{2}V}{L\omega} \left(\frac{2B_N + B_S - B_S}{B_N} \right) = \frac{2\sqrt{2}V}{L\omega}. \tag{4}$$

Assume that the air core impedance is about two times of transformer leakage impedance U_k[19]. The maximum peak of inrush current could then be expressed as

$$i_{\mathrm{peak}} \leq \frac{2\sqrt{2}V}{2U_k} = \sqrt{2} \left(\frac{V}{U_k} \right). \tag{5}$$

Then the relationship describing maximum peak value of inrush current and short-circuit impedance in the per unit system is

$$i_{\mathrm{peak}}{}^{(\mathrm{p.u.})} \leq \frac{\sqrt{2}}{\%U_k}. \tag{6}$$

Since the proposed relay utilizes rms values to calculate the differential currents, the maximum rms value of inrush current should be determined. The inrush current amplitude is almost zero for some duration of power frequency cycle [22]. Through precise calculation and practical recommendations [6], it is found that the maximum rms value of inrush current is less than 35% of the peak value. Therefore, the fundamental component of maximum possible inrush current for the power transformer under study is calculated by

$$I_{\rm rms} = 0.35 \times \frac{\sqrt{2}}{\%U_k} = 0.35 \times \frac{\sqrt{2}}{16.5\%} = 3^{(\rm p.u.)}. \qquad (7)$$

Therefore, considering a suitable safety margin to improve security of the relay and also to be compatible with Region-3, the upper limit of the Inrush-Region is set to 3.5 p.u.

F. Region Division Strategy

Region division strategy is a compromise between the setting simplification and adaptive operation time considering the fault severity and its influence on the power system. The main idea of region division is valid for different transformers. In addition, the general shape of the regions does not change considerably for a new high voltage power transformer. The borders of the regions and the required settings might have a minor change based on the studied transformer. Based on the conventional dual-slope differential relay characteristic, a strategy to define the regions and their borders is considered, as follows:

1) Region-1: The right hand side and bottom borders of this region are roughly fixed and selected based on the dual-slope differential relay characteristic. Meanwhile, the boundary between Region-1 and Region-2 is concluded from several simulations of mild internal faults. It is recommended that this boundary is set based on the junction point, JP in Fig. 2.

2) Inrush-region: Inrush current can be detected, even for a loaded transformer, by the proper selection of the Inrush-Region width. Although loaded transformer energization is not a common practice, it may occur when an auxiliary transformer is directly connected at the power transformer secondary side and thus they are both energized simultaneously. To consider such a case, the Inrush-Region width is set to 0.1 p.u.

3) Region-3: To accurately determine the Region-3 setting, a number of simulation cases including: 1) heavy saturation of some CTs due to external faults, and 2) severe inrush currents caused by transformer energization should be studied. For the studied system in the paper, the threshold of 3.5 p.u. is determined based on such simulation studies. Meanwhile, the threshold can be roughly considered equal to $1/U_k$. Although this is higher than the accurately determined setting, it guarantees the relay stability against both inrush current and severe CT saturation.

4) Region-2: This region is surrounded by the other regions while the right hand side border of this region is fixed based on the second slope of the differential relay characteristic.

5) CTSDEF-Region: The bottom border of this region is fixed, while the left hand side border is determined using the dual-slope characteristic.

IV. Adaptive Decision Logic

A. Weighting Factors of the Regions

When the current trajectory enters into the relay operational zone, a WF is adopted to it depending upon its region. For the case of low and medium differential currents, usually there is no risk of power system instability. In this condition, the trajectory of differential current lies inside Region-1 and due to the lower amount of fault current, very fast operation of the proposed relay is not vital. Therefore, the lowest WF, 1.8, is assigned to Region-1.

On the other hand, high differential currents enter Region-2 and therefore, a moderate WF value, that is, 3 is assigned to this region. Meanwhile, Region-2 is affected by CT saturation, so the WF of this region is adaptively controlled by CTSDEF-Region. If CT saturation for an external fault is detected and then the current trajectory moves into Region-2 or Region-1, the proposed relay must be blocked. Therefore, if the current enters into CTSDEF-Region and then lies in Region-2 or Region-1, the WFs of both regions will be scaled down by an appropriate factor to stabilize the proposed relay. This factor is determined in Section V-B. When the current trajectory leaves Region-2 or Region-1, the WFs are reset to the default values. Utilizing CTSDEF-Region guarantees stability of the proposed relay for external faults. Meanwhile the relay provides fast operation for simultaneous internal faults.

The maximum WF, 5, is assigned to Region-3 to cope with severe internal faults. The amplitude of inrush current can be as high as internal fault current and its trajectory can enter the operational zone. Hence, Inrush-Region with $\mathrm{WF} = 0$ is utilized to block the proposed relay in the case of inrush phenomenon.

B. Proposed Algorithm

The differential and restraint currents for three phases are calculated for each new sample. When each of the current trajectories enters into its operating region, the appropriate weighting factor is adopted. Afterwards, the cumulative weighting factor $\mathrm{W_x}$ for each phase, which is the sum of WFs is calculated using

$$W_x = \sum_{j=1}^{N} (\mathrm{WF}_x)_j \qquad x = A, B, C \qquad (8)$$

where N is the number of successive calculated WFs.

To expedite the relay operation, especially for a multiphase fault, a combined weighting factor strategy is used. In such a strategy, when two or three current trajectories enter into their associated operating regions, the sum of the cumulative weighting factors is considered as the total weighting factor.

$$W_{\rm Total} = \sum_{x=A,B,C} W_x. \qquad (9)$$

The block diagram of the proposed relay is depicted in Fig. 8. After calculating the current phasors, elimination of the zero sequence component and compensation of the vector group, the differential and restraint currents are calculated. Based on the position of the currents in the relay characteristic regions, a WF is adopted for each phase. Afterwards, the cumulative WF for each phase and finally the total WFs are calculated. The obtained

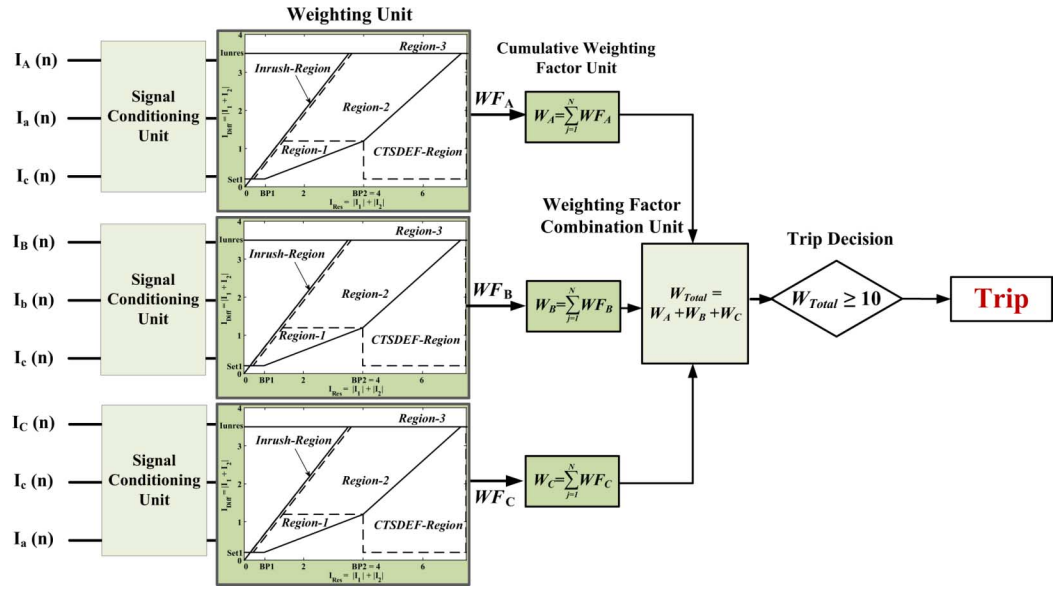

Fig. 8. Block diagram of the proposed algorithm.

value is compared with the set-value of 10 to activate the relay trip command.

C. Adaptive Division of Inrush Region

It is likely that an internal fault occurs during energization of a power transformer. In this condition, the current trajectory enters into Inrush-Region. In general, the inrush current has a decaying characteristic, i.e., the amplitude of the inrush current declines after its initiation. However, incident of an internal fault increases the current amplitude. Therefore, based on this concept, an adaptive division of Inrush-Region is applied to distinguish internal faults during switching on a power transformer.

The Inrush-Region is divided by a horizontal adaptive line into two sections shown in Fig. 9. It should be noted that the worst conditions are considered to calculate the maximum inrush current by (7), but the inrush current amplitude is often less than this value, in practice. Based on the initial magnitude of the inrush current, the threshold is selected adaptively. The amplitude of this adaptive threshold is 1.1 times of the first cycle of inrush current. The underneath part is the restraint section with WF = 0 and the upper one, is the operating section with WF = 3.

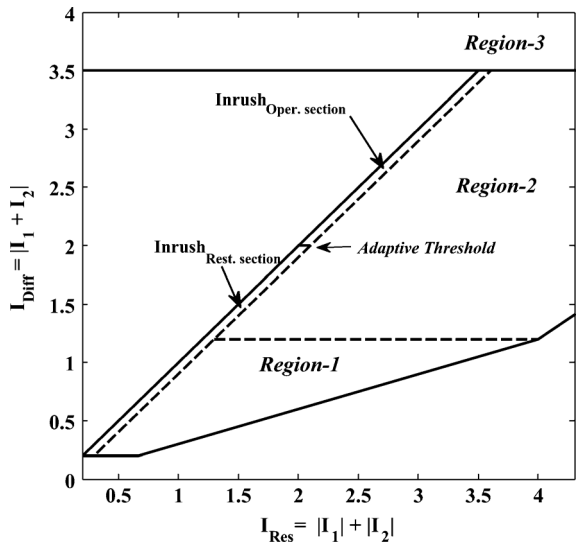

Fig. 9. Two sections of Inrush-Region.

V. Evaluation of the Proposed Approach

To investigate the merits of the proposed algorithm, various time-domain simulation studies are performed. To provide more realistic results, 3% white noise is added to the simulation signals of the studied system. Then, the signals are analyzed by the proposed adaptive regional differential relay.

A. Internal Faults

To investigate the relay performance for a mild internal fault, a phase-to-ground fault at 15% of phase-A winding is studied. Fig. 10 illustrates the differential relay current trajectories for the three phases. In this case, Region-1 of phase-A is activated. The proposed approach operates 17 ms after fault inception; whereas, the conventional relay issues the trip command after 21 ms.

The current trajectories for a phase-to-phase fault at the LV terminals of a and c phases are illustrated in Fig. 11. Due to the fault resistance of 20Ω, the fault currents are limited. According to Fig. 11, current trajectories enter Region-1 of all three phases and Region-2 of phase-A which results in the relay operation of 13 ms after fault inception. The conventional relay operates after 23 ms in this case.

Using the CTSDEF concept does not prevent fast operation of the proposed relay in the case of simultaneous CT saturation and internal fault. For instance, a phase-to-phase fault at the LV terminals of a and b phases is simulated at 500 ms while phase-A CT core includes 90% remanent flux. Fig. 12 shows the primary and secondary currents of phase-A, in which the CT of phase-A is saturated at 509 ms. The current trajectory of phase-A, shown

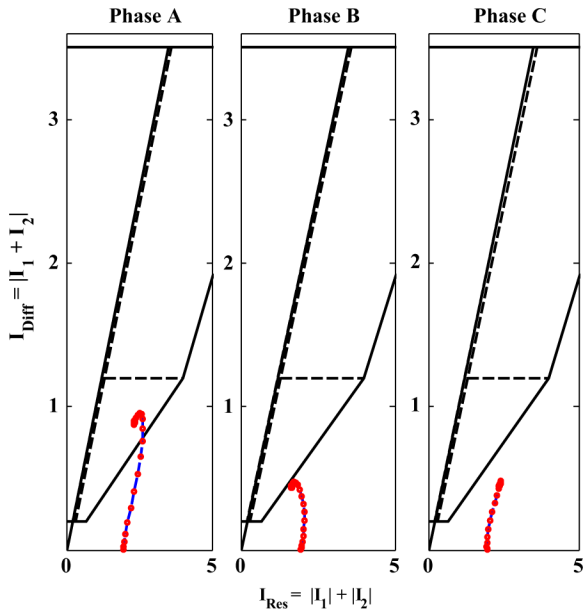

Fig. 10. Current trajectories for an AG internal fault at 15% of phase-A winding.

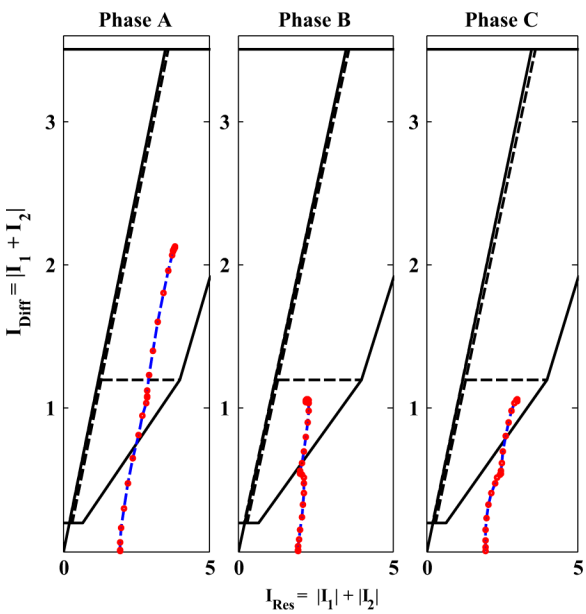

Fig. 11. Current trajectories for a phase-to-phase fault at the terminals of a and c phases, $\mathrm{Rf} = 20\Omega$.

in Fig. 13, enters Region-1 at 505 ms. The proposed relay detects this internal fault quite fast while phase-A CT is saturated.

B. External Fault With CT Saturation

In order to study stability of the proposed relay in the case of CT saturation, various external fault types with different amounts of CT core remanence were simulated. A typical case is presented below in detail.

A three phase fault at the LV terminals is simulated at 500 ms while phase-A CT core includes 90% remanent flux. The

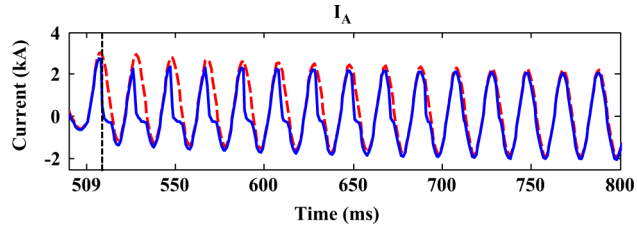

Fig. 12. Primary and secondary currents of phase-A for a phase-to-phase fault at the LV terminals of a and b phases.

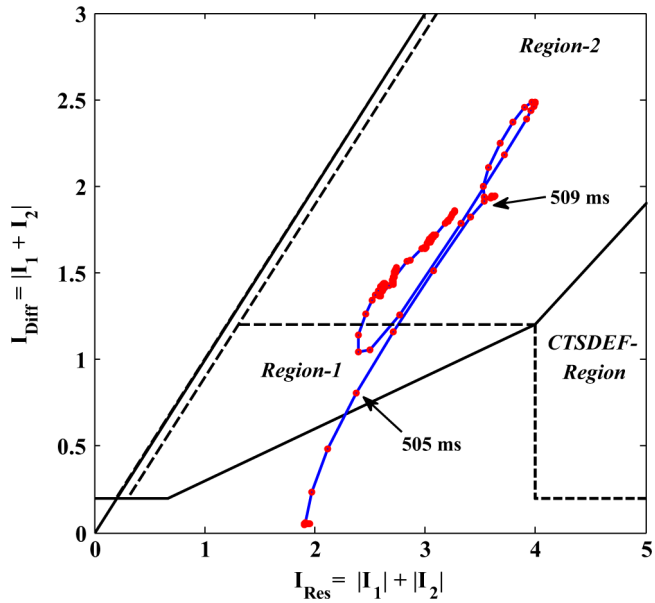

Fig. 13. Current trajectory of phase-A for the case depicted in Fig. 12.

primary and secondary currents of high voltage side and differential characteristic of phase-A are shown in Figs. 14 and 15, respectively. The CT saturation occurs at 508 ms and CTSDEF-Region is activated during 509 ms to 529 ms. The current trajectory enters into Region-2 of phase-A at 530 ms while the proposed algorithm sets WF of Region-2 to 0.01 from 530 ms to 575 ms, when the current trajectory leaves Region-2. As a result, the proposed relay does not maloperate for this external fault.

C. Internal Fault Following Inrush Current

The performance of the proposed relay is examined for a combinational case. The transformer is switched on at 300 ms and later an internal fault at 20% of phase-A winding occurs at 500 ms. High voltage side line currents and also activation signal of Inrush-Region are shown in Fig. 16. As shown, inrush condition is detected at 310 ms when the current trajectory enters the restraint section of Inrush-Region. Based on phasor estimation of the first cycle of inrush current, the calculated adaptive thresholds of phase-A, phase-B and phase-C are 0.5, 0.26, and 0.26 p.u., respectively. After internal fault inception, differential currents increase and become more than the adaptive thresholds. Under such a condition, the differential current trajectories enter the operating section of Inrush-Regions at 508

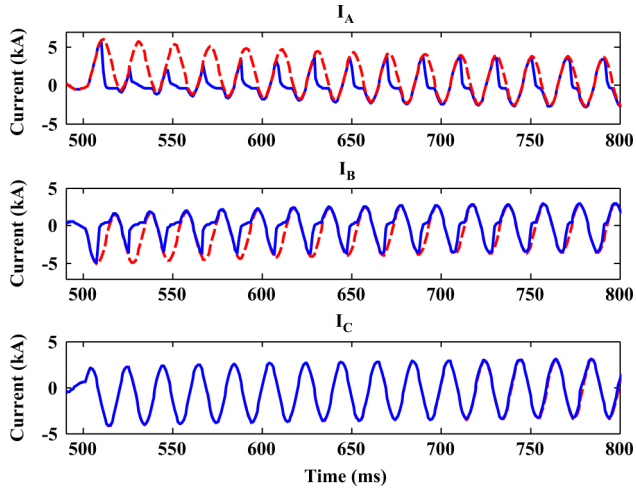

Fig. 14. Primary and secondary currents of high voltage side for a three phase external fault with 90% core remanence.

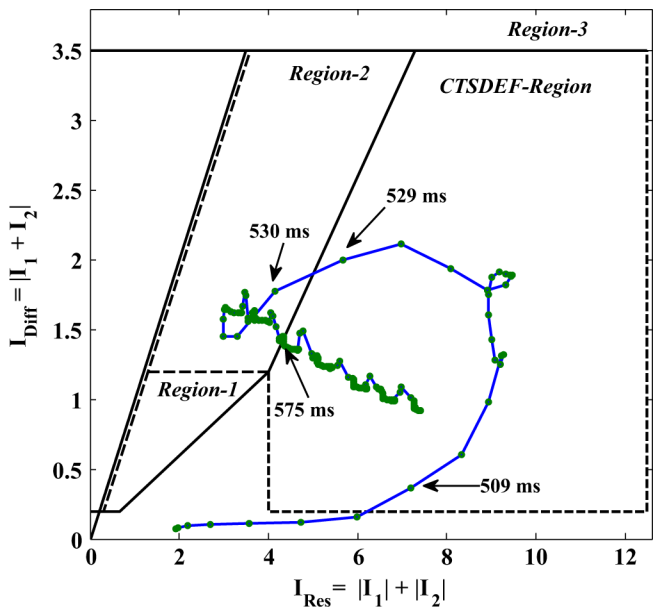

Fig. 15. Current trajectory of phase-A for the case depicted in Fig. 14.

ms, thus the trip signal is issued at 509 ms. It shows proper operation of the proposed adaptive relay for this combinational case.

VI. Comparing Proposed and Conventional Approaches

Many of the commercial relays utilize the second harmonic component to block the differential relay against inrush current. Sudden current change and decaying dc component of the fault current generate a large amount of the second harmonic component which can block these relays for about 15 ms after the fault inception [28]. Meanwhile, a fix time delay, for example, 4 ms [24], [25] is usually used to ensure occurrence of an internal fault. Accordingly, the trip command is issued about one cycle after the fault instant. The proposed approach not only decreases the intentional time delay by utilizing the adaptive weighting-based technique, but also is not directly blocked by the inrush detection unit. Consequently, this approach operates faster than the conventional differential relays.

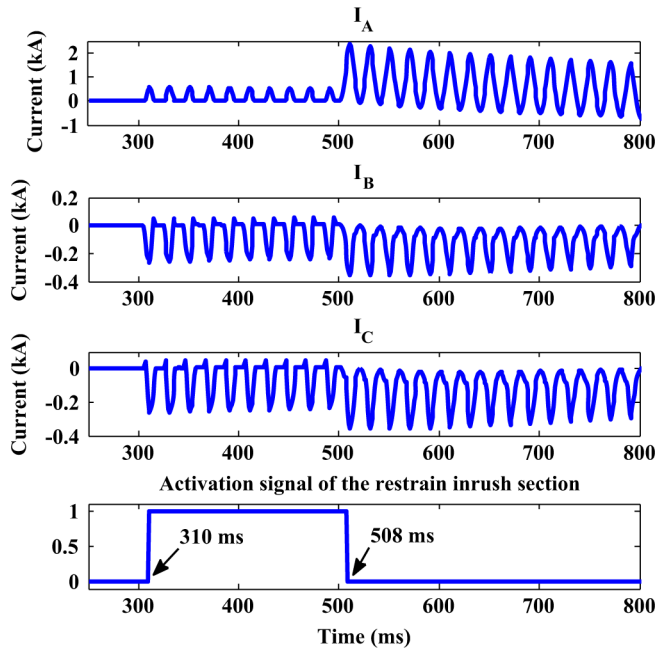

Fig. 16. HV line currents and activation signal of the restrain inrush section, internal fault occurrence after energizing a power transformer.

TABLE I
Proposed Relay Operation Time for Internal Faults

Fault type	R_f *(Ω)*	R_1	R_2	R_3	*Operating time (ms)*	
					Proposed approach	*Conventional approach*
AG-15%	0	√	×	×	17	19
AG-25%	0	√	√	×	12	19
AG-25%	5	√	√	×	16	23
AG-30%	0	√	√	×	11	19
AG-30%	5	√	√	×	14	23
AG-30%	10	√	√	×	19	23
AB	0	×	√	√	4	17
AB	20	×	√	√	4	21
ABC	0	√	√	√	4	10
ac-2%	0	√	√	×	15	19
ac-10%	0	√	√	×	9	19
ac	0	√	√	√	7	19
abc	0	√	√	√	5	20
Inrush &ABC	0	√	√	√	4	20
Inrush & ac	0	√	√	√	6	19
Inrush & AG	0	√	√	√	5	156
Inrush & AG-15%	0	√	√	×	9	123

Capital letters denote high voltage side, lower case letters indicate low voltage side, and R_X denotes activation of Region-x.

Performance of the proposed approach as compared with that of the conventional differential relay for various internal faults and system disturbances is summarized in Table I. The last four cases indicate occurrence of an internal fault after the inrush current. It shows that in most cases, the operation time of the proposed differential relay is lower for about a quarter-cycle.

Moreover, the approach issues the trip command much faster than the conventional relay in the case of an internal fault following an inrush current.

VII. Conclusion

A new adaptive multiregion differential relay for power transformers is proposed in this paper. Based on current trajectory and fault condition, the operational zone of relay characteristic is divided into three operating regions. Internal faults are detected by conventional differential relays, while the current trajectory remains in the operational zone of low impedance characteristic for a certain time. But in the proposed relay this fix time is adaptively changed through a weighting procedure. A weighting factor is adopted to the current trajectory signals of each phase according to associated region, in which higher weights are considered for the faults with a higher degree of certainty. Afterwards, the cumulative WF of three phases is utilized to send trip command.

In addition, two control regions (Inrush-Region and CTSDEF-Region) are utilized to stabilize relay in the case of inrush current and CT saturation to adapt WF of operating regions. Internal faults incorporated with inrush current are detected by adaptive division of the Inrush-Region.

The simulation studies show that the proposed adaptive logic is able to improve the differential relay performance and increase the relay flexibility in adaption to the fault condition. The obtained results indicate that the proposed approach can accelerate the relay operation in internal faults. Also it can stabilize the differential relay in the non-faulty conditions.

Appendix

The parameters of the 230 kV system used for the simulation studies are as follows.

a) Equivalent source: $V_{Th} = 230$ kV, $Z_{Th} = 0.553 + j11.05\Omega$

b) Power transformer parameters: YNd11, core-type three-phase, $V_1 = 230$ kV, $V_2 = 63$ kV $S_n = 160$ MVA, $\%U_k = 16.5\%$

References

[1] M. J. Heathcote, *The J & P transformer book,A Practical Technology of the Power Transformer*, 13th ed ed. Oxford, U.K.: Elsevier Sci. Technol. Books, 2007.

[2] L. Pei, O. P. Malik, C. Deshu, G. S. Hope, and G. Yong, "Improved operation of differential protection of power transformers for internal faults," *IEEE Trans. Power Del.*, vol. 7, no. 4, pp. 1912–1919, Oct. 1992.

[3] A. Guzman, N. Fischer, and C. Labuschagne, "Improvements in transformer protection and control," in *Proc. 62nd Protect. Relay Eng. Annu. Conf.*, 2009, pp. 563–579.

[4] S. Myong-Chul, P. Chul-Won, and K. Jong-Hyung, "Fuzzy logic-based relaying for large power transformer protection," *IEEE Trans. Power Del.*, vol. 18, no. 3, pp. 718–724, Jul. 2003.

[5] L. Yang, "An approach to identify magnettizing inrush currents and its simulation," in *Proc. Electron. Mech. Eng. Inf. Technol. Int. Conf.*, 2011, pp. 2377–2380.

[6] G. Ziegler, *Numerical Differential Protection, Principles and Applications*. Erlangen, Germany: Publicis Corporate Publishing, 2005.

[7] J. Pihler, B. Grcar, and D. Dolinar, "Improved operation of power transformer protection using artificial neural network," *IEEE Trans. Power Del.*, vol. 12, no. 3, pp. 1128–1136, Jul. 1997.

[8] M. R. Zaman and M. A. Rahman, "Experimental testing of the artificial neural network based protection of power transformers," *IEEE Trans. Power Del.*, vol. 13, no. 2, pp. 510–517, Apr. 1998.

[9] A. L. Orille-Fernandez, N. K. I. Ghonaim, and J. A. Valencia, "A firann as a differential relay for three phase power transformer protection," *IEEE Trans. Power Del.*, vol. 16, no. 2, pp. 215–218, Apr. 2001.

[10] A. Wiszniewski and B. Kasztenny, "A multi-criteria differential transformer relay based on fuzzy logic," *IEEE Trans. Power Del.*, vol. 10, no. 4, pp. 1786–1792, Oct. 1995.

[11] A. Ferrero, S. Sangiovanni, and E. Zappitelli, "A fuzzy-set approach to fault-type identification in digital relaying," *IEEE Trans. Power Del.*, vol. 10, no. 1, pp. 169–175, Jan. 1995.

[12] B. Kasztenny, E. Rosolowski, M. M. Saha, and B. Hillstrom, "A self-organizing fuzzy logic based protective relay-an application to power transformer protection," *IEEE Trans. Power Del.*, vol. 12, no. 3, pp. 1119–1127, Jul. 1997.

[13] M. M. Eissa, "A novel digital directional transformer protection technique based on wavelet packet," *IEEE Trans. Power Del.*, vol. 20, no. 3, pp. 1830–1836, Jul. 2005.

[14] A. Ngaopitakkul and A. Kunakorn, "Internal fault classification in transformer windings using combination of discrete wavelet transforms and back-propagation neural networks," *Int. J. Control, Autom., Syst.*, vol. 4, no. 3, pp. 365–371, 2006.

[15] S. A. Saleh and M. A. Rahman, "Modeling and protection of a three-phase power transformer using wavelet packet transform," *IEEE Trans. Power Del.*, vol. 20, no. 2, pt. 2, pp. 1273–1282, Apr. 2005.

[16] M. Jing, W. Zengping, Y. Qixun, and L. Yilu, "Identifying transformer inrush current based on normalized grille curve," *IEEE Trans. Power Del.*, vol. 26, no. 2, pp. 588–595, Apr. 2011.

[17] A. Hooshyar, S. Afsharnia, M. Sanaye-Pasand, and B. M. Ebrahimi, "A new algorithm to identify magnetizing inrush conditions based on instantaneous frequency of differential power signal," *IEEE Trans. Power Del.*, vol. 25, no. 4, pp. 2223–2233, Oct. 2010.

[18] M. Sanaye-Pasand and P. Jafarian, "An adaptive decision logic to enhance distance protection of transmission lines," *IEEE Trans. Power Del.*, vol. 26, no. 4, pp. 2134–2144, Oct. 2011.

[19] P. Wilson, *User's Guide on the Use of PSCAD*, 3rd ed. Winnipeg, MB, Canada: Manitoba HVDC Reseach Center, 2004.

[20] P. Bertrand, A. Devalland, and P. Bastard, "A simulation model for transformer internal faults, base for the study of protection and monitoring systems," presented at the 12th Int. Conf. Elect. Distrib., Birmingham, U.K., 1993.

[21] J. Tellinen, "A simple scalar model for magnetic hysteresis," *IEEE Trans. Magn.*, vol. 34, no. 4, pt. 2, pp. 2200–2206, Jul. 1998.

[22] *"Technical Reference Manual of RET 521*2.3 (Transformer protection terminal),"* ABB, ABB Relay Catalogue-1MRK 504 016-UEN.

[23] *"Manual of SIPROTEC 7UT612 (Differential Protection),"* Siemens, Siemens relay catalogue.

[24] *"Application Manual of RET670 (Transformer Protection Relay),"* ABB, ABB Relay Catalogue-1MRK 504 116-UEN.

[25] E. C. Segatto and D. V. Coury, "A differential relay for power transformers using intelligent tools," *IEEE Trans. Power Syst.*, vol. 21, no. 3, pp. 1154–1162, Aug. 2006.

[26] *"Technical Manual of P632, P633, P634 (Transformer Differential Protection),"* AREVA relay catalogue-P63x/UK M/A54 p. 631.

[27] N. Chiesa, B. A. Mork, and H. K. Hoidalen, "Transformer model for inrush current calculations: simulations, measurements and sensitivity analysis," *IEEE Trans. Power Del.*, vol. 25, no. 4, pp. 2599–2608, Oct. 2010.

[28] C. H. Einval and J. R. Linders, "A three-phase differential relay for transformer protection," *IEEE Trans. PAS*, vol. PAS-94, no. 6, pt. 1, pp. 1971–1980, Nov./Dec. 1975.

Hamed Dashti received the M.Sc. degree in electrical engineering from the University of Tehran, Tehran, Iran, in 2007, where he is currently pursuing the Ph.D. degree in electrical engineering.

Majid Sanaye-Pasand (M'98–SM'05) received the M.Sc. and Ph.D. degrees in electrical engineering from the University of Calgary, Calgary, AB, Canada, in 1994 and 1998, respectively.

Currently, he is a Professor with the School of Electrical and Computer Engineering, University of Tehran, where he is also with the Control and Intelligent Processing Center of Excellence.